Available online at www.sciencedirect.com

ScienceDirect

Journal of Materiomics 1 (2015) 188–195

www.ceramsoc.com/en/

www.journals.elsevier.com/journal-of-materiomics/

Orientation and film thickness dependencies of (100)- and (111)-oriented epitaxial $Pb(Mg_{1/3}Nb_{2/3})O_3$ films grown by metal organic chemical vapor deposition

Hiroshi Funakubo [a,*], Satoshi Okamaoto [a], Shintaro Yokoyama [a], Shoji Okamoto [a], Junichi Kimura [a], Hiroshi Uchida [b]

[a] *Department of Innovative and Engineered Materials, Tokyo Institute of Technology, Yokohama 226-8502, Japan*
[b] *Department of Materials and Life Sciences, Sophia University, Tokyo 102-8554, Japan*

Received 30 May 2015; revised 27 June 2015; accepted 6 July 2015
Available online 23 July 2015

Abstract

(100)- and (111)-oriented epitaxial $Pb(Mg_{1/3}Nb_{2/3})O_3$ films with 500 and 1300 nm in thickness were grown by metal organic chemical vapor deposition. Remained strain was almost relaxed because the crystal structure of the films was almost the same as that of bulk $Pb(Mg_{1/3}Nb_{2/3})O_3$. Relative dielectric constant showed the maximum value against the temperature that depended on the measurement frequency. Maximum relative dielectric constant, ε_r(max.), and the temperature showing ε_r(max.), T(max.), decreased and increased with the frequency, respectively, are in good agreement with reported data for the bulk. ε_r(max.) and T(max.), respectively increased and decreased with the film thickness and (111)-oriented films showed larger value than that of the (100)-oriented one. Ferroelectricity was observed for all films up to 297 K and monotonously decreased with increasing temperature. Saturation polarization value increased with the film thickness and (111)-oriented films showed larger value than (100)-oriented ones. On the other hand, the coercive field decreased with increasing film thickness, but was almost independent with the film orientation.

Keywords: $Pb(Mg_{1/3}Nb_{2/3})O_3$ epitaxial film; Thickness dependency; Orientation dependency; Dielectric property; Ferroelectric property

1. Introduction

$Pb(Mg_{1/3}Nb_{2/3})O_3$ (PMN) is one of well-known relaxor ferroelectric materials with diffused phase transition [1]. This is also known as an end member of $Pb(Mg_{1/3}Nb_{2/3})O_3$–$PbTiO_3$ solid solution system that has been widely investigated for capacitor and piezoelectric transducer applications due to its large dielectric constant and piezoelectric properties near the morphotropic phase boundaries, respectively [2]. Film form of $Pb(Mg_{1/3}Nb_{2/3})O_3$–$PbTiO_3$ solid solution has been also investigated for the applications in high density capacitors and microelectromechanical system (MEMS) using piezoelectric materials, so called piezo-MEMS [3]. However, the number of researches for $Pb(Mg_{1/3}Nb_{2/3})O_3$ films itself is relatively small compared with $Pb(Mg_{1/3}Nb_{2/3})O_3$–$PbTiO_3$ solid solution films.

Seo et al. [4] reported that the crystal structure changes with film thicknesses from 35 to 370 nm for (100)-oriented $Pb(Mg_{1/3}Nb_{2/3})O_3$ epitaxial films. On the other hand, *Nagarajan* et al. reported the strong film thickness dependency of the lattice parameter for 10% $PbTiO_3$ substituted (100)-oriented $Pb(Mg_{1/3}Nb_{2/3})O_3$ epitaxial films from 100 to 400 nm in thickness [5]. They explain this dependence by the strain effect from the substrate. However, the investigation on the film thickness

* Corresponding author. Tokyo Institute of Technology, J2-43, 4259, Nagatsuta-cho, Midori-ku Yokohama, Kanagawa 226-8502, Japan.
E-mail addresses: funakubo.h.aa@m.titech.ac.jp (H. Funakubo), uchidah@sophia.ac.jp (H. Uchida).
Peer review under responsibility of The Chinese Ceramic Society.

http://dx.doi.org/10.1016/j.jmat.2015.07.004

dependency beyond 1000 nm in thickness has been hardly reported. Our group reported the strong film thickness dependency of the dielectric constant, ε_r, for wide range of film thickness from 100 nm to 2000 nm [6]. This is different from previous reports because the obvious strain change with film thickness was not detected by the relaxation of the remained strain mainly due to the relatively thick film. In addition, this strong film thickness dependency of ε_r cannot be explained by the widely discussed so-called "dead-layer model'' [7]. In this model, the inverse of the capacitance has a linear relationship with film thickness having a positive intercept value at 0 nm in thickness. However, a linear relationship was not obtained in our previous study. One possibility to explain the strong film thickness dependency of ε_r observed in the previous study is the change of the temperature dependency of ε_r with film thickness because ε_r was previously measured at the fixed temperature, room temperature.

On the other hand, orientation dependencies of the dielectric and ferroelectric properties have been reported for various ferroelectric films [8,9]. This is because ferroelectric materials have polar characteristics. However, the film orientation dependency has been hardly reported for $Pb(Mg_{1/3}Nb_{2/3})O_3$ films.

In the present study, (100)- and (111)-oriented epitaxial $Pb(Mg_{1/3}Nb_{2/3})O_3$ films with different film thickness were grown by metal organic chemical vapor deposition (MOCVD) and temperature dependencies of the dielectric and ferroelectric properties were systematically investigated for the first time.

2. Experimental procedure

$Pb(Mg_{1/3}Nb_{2/3})O_3$ films with 500 and 1300 nm in thickness were grown on $(100)_cSrRuO_3//(100)SrTiO_3$ and $(111)_cSrRuO_3//(111)SrTiO_3$ substrates at 650 °C by pulsed MOCVD. The details on the pulsed MOCVD have already been reported elsewhere [10]. $Pb(C_{11}H_{19}O_2)_2$, $Mg(C_{14}H_{25}O_2)_2$ (Asahi Denka Corp.) and $Nb(OC_2H_5)_5$ were respective used as

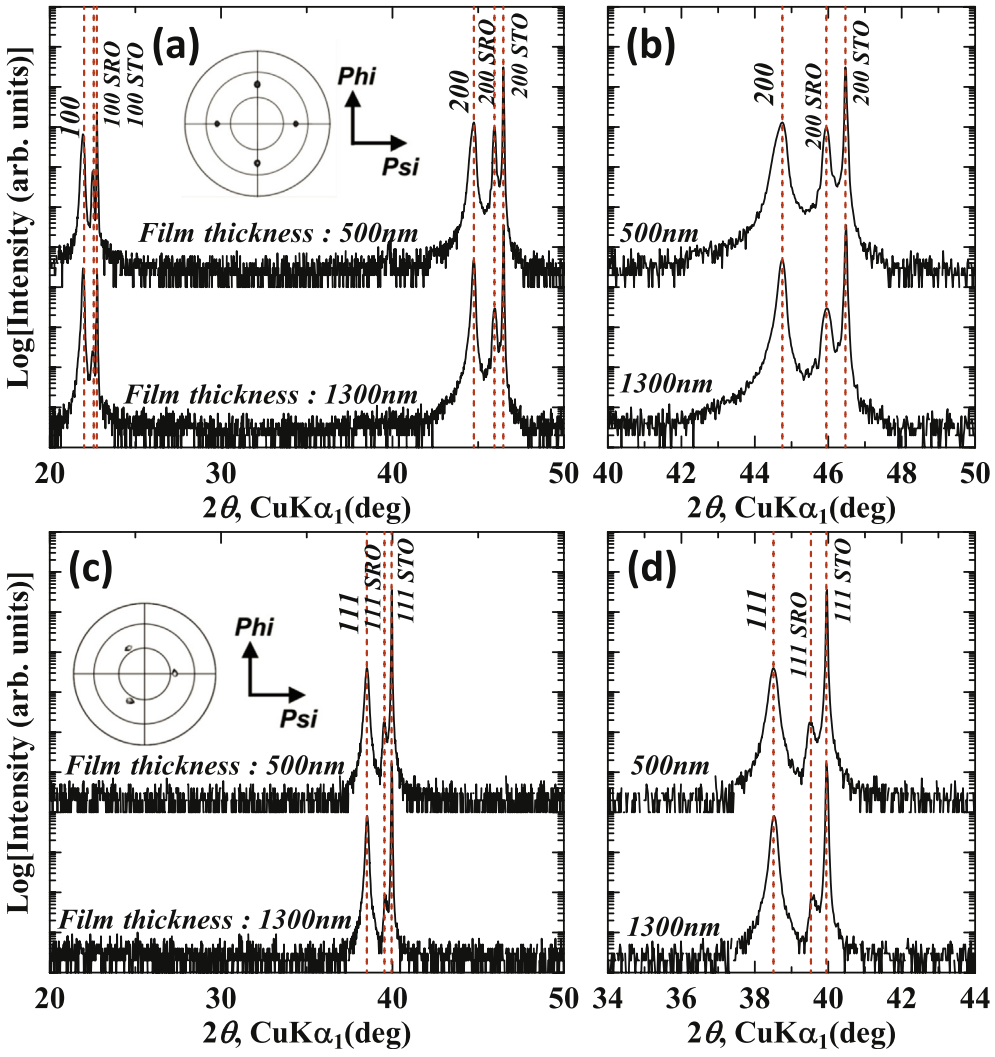

Fig. 1. XRD θ -2θ scan data for 500 nm and 1300 nm thick films grown on (a, b) $(100)_cSrRuO_3//(100)SrTiO_3$ substrates and (c, d) $(111)_cSrRuO_3//(111)SrTiO_3$ substrates. (b) and (d) respective show the enlarged ones of (a) and (c) near $SrTiO_3$ *200* and *111*. X-ray pole figures measured at fixed 2θ angle corresponding to $Pb(Mg_{1/3}Nb_{2/3})O_3$ *101* for 1300 nm thick films are shown as inserted figures.

Pb, Mg and Nb source materials. Oxygen and nitrogen gasses were used as the oxidant and the carrier gas, respectively. The source gas mixture flowed to the substrates in a cold-wall-type vertical reaction chamber. Pb/(Pb + Mg + Nb) ratio was kept to be 0.5 by controlling the concentration ratio of the input source gasses under a constant Mg/(Mg + Nb) = 0.33. Film thickness was controlled by adjusting both deposition time and deposition rate.

Epitaxial $SrRuO_3$ films were used as bottom electrode and were grown on (100) and (111) $SrTiO_3$ substrates at 750 °C by MOCVD using $Sr(C_{11}H_{19}O_2)_2(C_8H_{23}N_5)_2$, $Ru(C_7H_{11})(C_7H_9)$ (TOSOH Corp.) and oxygen as sources [11]. The pseudo-cubic Miller index of the crystal, designated in brackets as $(hkl)_c$, is used for $SrRuO_3$. The resultant substrates were $(100)_cSrRuO_3//(100)SrTiO_3$ and $(111)_cSrRuO_3//(111)SrTiO_3$.

The crystal structure of the deposited films was investigated using X-ray diffraction (XRD; PANalytical X'Pert MRD) analysis. To characterize the electrical properties of the deposited films, 100-μm-diameter Pt top electrodes were deposited by electron-beam evaporation using a shadow metal mask. Dielectric and ferroelectric properties were measured at room temperature with an HP4194A impedance analyzer and ferroelectric tester (TOYO Corp. FCE), respectively. The temperature dependence of the electrical properties was measured using a probing system with a temperature-controlled stage.

3. Results and discussion

3.1. Crystal structure at room temperature

Fig. 1 shows the XRD $\theta - 2\theta$ scan data for the obtained films. Only *h00* diffraction peaks were observed for both of 500 and 1300 nm thick films grown on $(100)_cSrRuO_3//(100)SrTiO_3$ substrates as shown in Fig. 1(a). On the other hand, only *111* diffraction peak was observed in the 2θ range between 20 and 50° for both of 500 and 1300 nm thick films grown on $(111)_cSrRuO_3//(111)SrTiO_3$ substrates as shown in Fig. 1(c). In-plane aligned epitaxial growth of these films were ascertained by X-ray pole figure measurement as shown in the insets in Fig. 1(a) and (c) as follows: (100) $Pb(Mg_{1/3}Nb_{2/3})O_3//(100)_cSrRuO_3//(100)SrTiO_3$ and (111)$Pb(Mg_{1/3}Nb_{2/3})O_3//(111)_cSrRuO_3//(111)SrTiO_3$.

Fig. 1(b) and (d) show the enlarged $\theta - 2\theta$ scans near $Pb(Mg_{1/3}Nb_{2/3})O_3$ *200* and *111* for $Pb(Mg_{1/3}Nb_{2/3})O_3$ films grown on $(100)_cSrRuO_3//(100)SrTiO_3$ and $(111)_cSrRuO_3//(111)SrTiO_3$ substrates, respectively. No obvious peak shift with film thickness were detected for both oriented films.

Fig. 2 shows the estimated lattice parameters and the unit cell volume as a function of the film thicknesses for (100)- and (111)-oriented films. Lattice parameters of the deposited films were estimated by the X-ray reciprocal space mappings near $SrTiO_3$ *004* and *204*, and $SrTiO_3$ *222*, *224* and *114* for (100)-

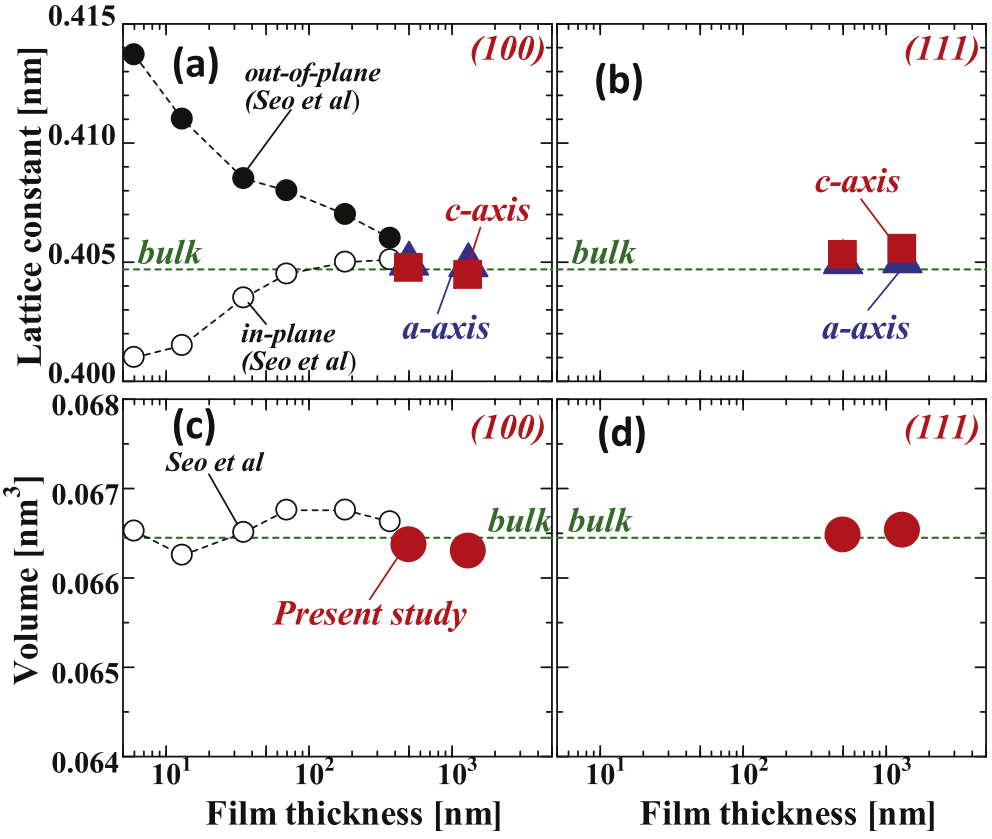

Fig. 2. (a, b) Lattice constants and (c, d) unit cell volume of films as a function of film thickness for $Pb(Mg_{1/3}Nb_{2/3})O_3$ films grown on (a, b) $(100)_cSrRuO_3//(100)SrTiO_3$ substrates and (c, d) $(111)_cSrRuO_3//(111)SrTiO_3$ substrates. Reported data from Ref. [4], Appl. Phys. Lett., 2004; 84: 3133–3135., are also shown in the figure together with the reported bulk $Pb(Mg_{1/3}Nb_{2/3})O_3$ data from [12], Sov. Phys. Crystallogr., 1960; 5: 292.

Table 1
Summary of lattice parameter.

Film thickness (nm)	(100) orientation		(111) orientation	
	a-axis (nm)	*c*-axis (nm)	*a*-axis (nm)	*c*-axis (nm)
500	0.4049	0.4048	0.405	0.4053
1300	0.4049	0.4045	0.4038	0.4058

and (111)-oriented $Pb(Mg_{1/3}Nb_{2/3})O_3$ films, respectively. Obtained lattice parameters are summarized in Table 1. Reported data for the bulk [12] and the (100)-oriented films [4] are also shown in Fig. 2. Obtained data in the present study almost agreed with the bulk data. These are reasonable taking account of the film thickness dependency of the lattice parameters as shown in Fig. 2(a) that the deviation of the lattice parameters from the bulk values decreased with the film thickness and then lattice parameters became almost constant with the bulk ones above 400 nm in thickness. This means that the remained strain in the film was relaxed with increasing film thickness and became almost the same value as that of bulk. The data shown in Fig. 2 suggest that the remained strain does not strongly contribute to the electrical properties of the deposited $Pb(Mg_{1/3}Nb_{2/3})O_3$ films in the present study as discussed in Section 3.2.

It must be mentioned that the refractive index of these films measured by spectroscopic ellipsometry was almost similar to the reported data of bulk $Pb(Mg_{1/3}Nb_{2/3})O_3$ [13]. This suggests that the density of the films is almost equivalent to the bulk one.

3.2. Dielectric property

Fig. 3 shows the temperature dependencies of the ε_r, and the dielectric loss, tanδ, measured at various frequencies for the films shown in Fig. 1. It must be noted that the vertical axis scales of Fig. 3(a) and (b) are different from those of Fig. 3(c) and (d), respectively, to show the details of the data. Clear orientation and film thickness dependencies were observed for both of ε_r and tan δ.

On the next step, typical characteristics of the data shown in Fig. 3 are summarized. Fig. 4 shows the frequency dependencies of the maximum ε_r, ε_r(max.), and temperature showing ε_r(max.), T(max.). Reported data of ε_r(max.) and T(max.) for the bulk $Pb(Mg_{1/3}Nb_{2/3})O_3$ are also shown in Fig. 4 [14]. ε_r(max.) decreased with increasing frequency irrespective of film thickness and the film orientations. However, this frequency dependency is smaller than reported data for the bulk one that is also ascertained for the normalized data by the ε_r(max.) at 10^2 Hz as shown in Fig. 5(a).

ε_r(max.) increased with increasing film thickness for both orientations irrespective of the frequency as shown in Fig. 4(a). However, this absolute value is still quite small compared with the reported data for the bulk. This suggests the strong film thickness dependency of ε_r(max.) at least up to 1300 nm. In fact, we already ascertained that ε_r at room temperature monotonously increased with film thickness up to 2000 nm [6]. Nagarajan et al. also reported the increase of ε_r(max.) with increasing film thickness for (100)-oriented epitaxial 0.9 $Pb(Mg_{1/3}Nb_{2/3})O_3$ − 0.1$PbTiO_3$ films up to

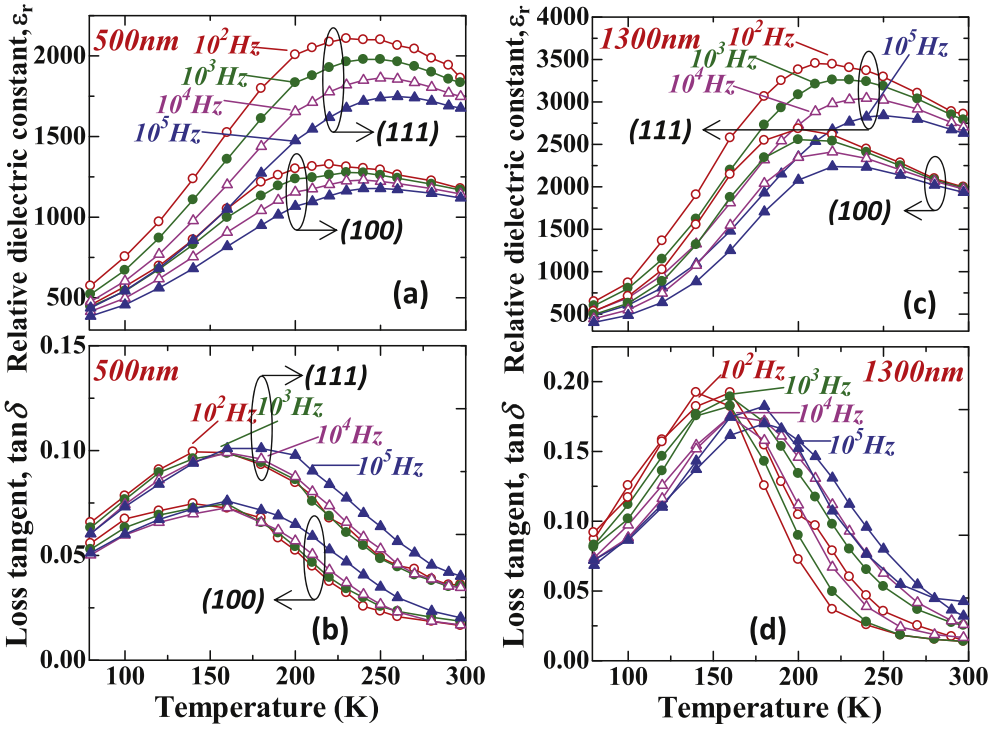

Fig. 3. Temperature dependencies of (a, b) the relative dielectric constant, ε_r, and (c, d) the dielectric loss, tanδ, measured at various frequency for the films shown in Fig. 1. (100): $Pb(Mg_{1/3}Nb_{2/3})O_3$ films grown on (100)$_c$$SrRuO_3$//(100)$SrTiO_3$ substrates (111): $Pb(Mg_{1/3}Nb_{2/3})O_3$ films grown on (111)$_c$$SrRuO_3$//(111)$SrTiO_3$ substrates.

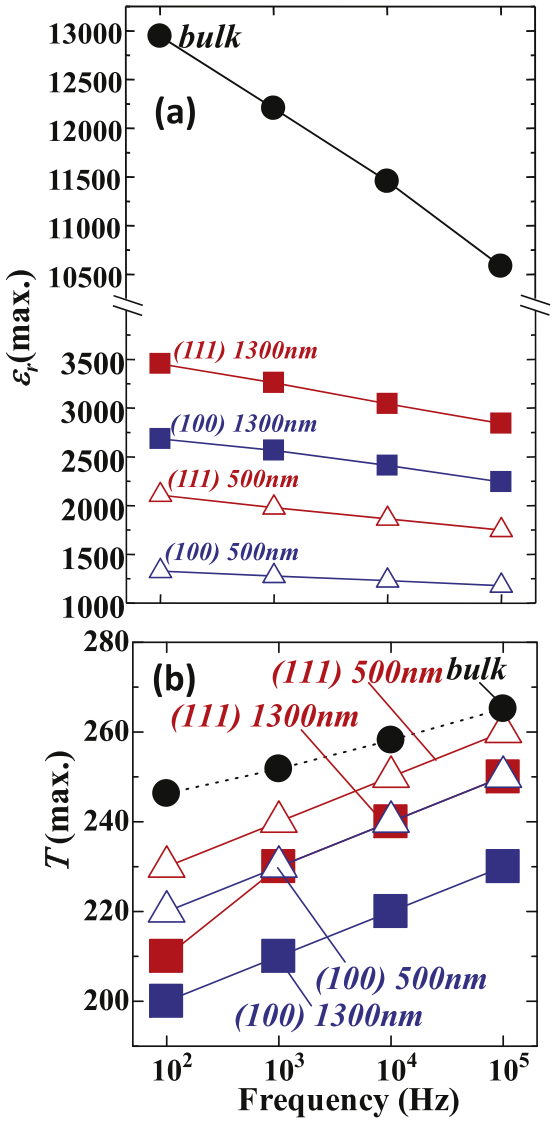

Fig. 4. Frequency dependencies of the maximum ε_r, ε_r(max.), and temperature showing ε_r(max.), T(max.) for 500 nm and 1300 nm thick $Pb(Mg_{1/3}Nb_{2/3})O_3$ films grown on $(100)_c SrRuO_3//(100)SrTiO_3$ and $(111)_c SrRuO_3//(111)SrTiO_3$ substrates.

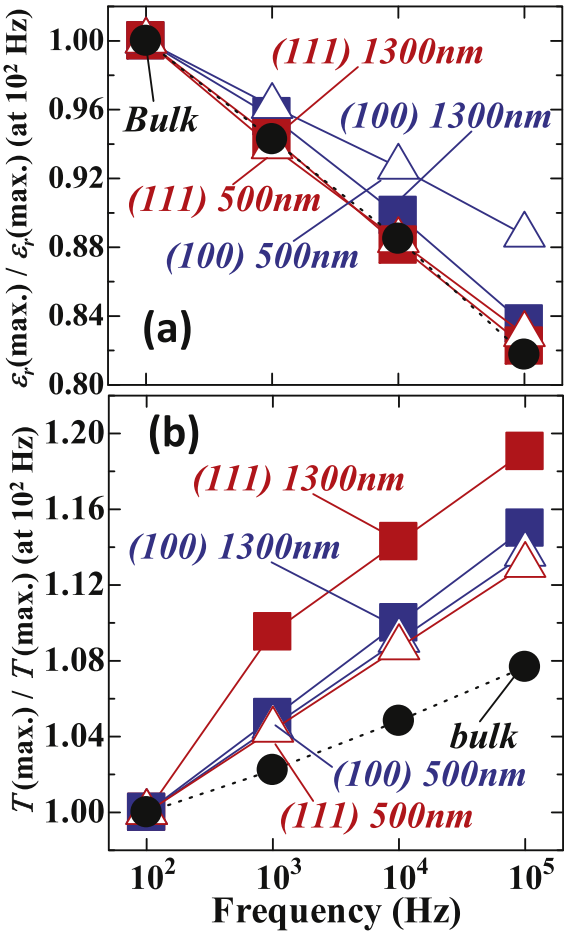

Fig. 5. ε_r(max.) and T(max.) normalized by the values at 10^2 Hz for 500 nm and 1300 nm thick $Pb(Mg_{1/3}Nb_{2/3})O_3$ films grown on $(100)_c SrRuO_3//(100)SrTiO_3$ and $(111)_c SrRuO_3//(111)SrTiO_3$ substrates.

400 nm in thickness [5]. One possible reason of the smaller ε_r(max.) of the $Pb(Mg_{1/3}Nb_{2/3})O_3$ films than that of $Pb(Mg_{1/3}Nb_{2/3})O_3$ single crystal is the lower process temperature of the film than that of the single crystal. Lower process temperature is possible to affect the size and the distribution of "micro polar regions" that is pointed out to control the dielectric properties of the relaxor ferroelectrics [1]. On the other hand, (111)-oriented films showed larger ε_r(max.) than (100)-oriented one for both film thicknesses in the present study. The crystallographic relationship is also reported for $Pb(Mg_{1/3}Nb_{2/3})O_3$ single crystal that ε_r value of (111) is larger than that of (100) one [15]. In addition, larger ε_r of (111)-oriented films than (100)-oriented ones is also reported for Pb(Zr, Ti)O_3 films [8,9]. This is considered to be due to the larger domain contribution of (111) orientation compared to (100) one as *Xu* et al. pointed out [9].

Fig. 4(b) shows the frequency dependency of T(max.) based on the data shown in Fig. 3 together with the reported bulk data [14]. T(max.) increased with increasing frequency for all films as same as the reported data for the bulk. This frequency dependency is larger than reported data for the bulk. This is clear for the normalized data by the T(max.) at 10^2 Hz as shown in Fig. 5(b).

T(max.) decreased with increasing film thickness for both orientations even if the reported bulk data is higher than the present study. Same trend of T(max.) which decreases with film thickness is also reported by *Nagarajan* et al. for (100)-oriented epitaxial 0.9 $Pb(Mg_{1/3}Nb_{2/3})O_3 - 0.1PbTiO_3$ films up to 400 nm in thickness [5]. This is also possible to explain by the low process temperature of the single crystal one. When you compare the orientation, T(max.) of (111)-oriented films was higher than that of (100)-oriented one.

3.3. Ferroelectric property

Fig. 6 shows the polarization – electric field ($P - E$) relationships measured at various temperatures. Clear hysteresis loops originating from the ferroelectricity were observed for all temperature range up to 297 K, especially for 500 nm thick films. It must be noted that 297 K is higher than T(max.) as discussed in Section 3.2.

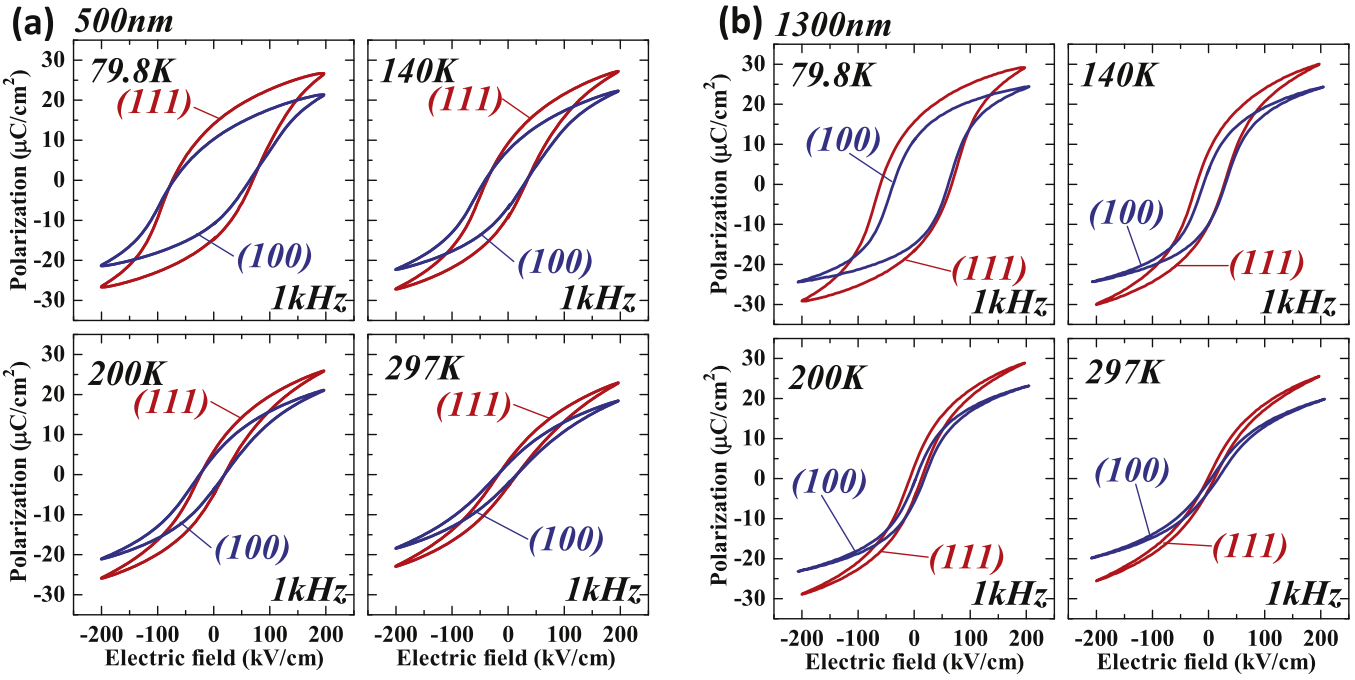

Fig. 6. Polarization–electric field (P–E) relationships measured at various temperature for (a) 500 nm and (b) 1300 nm-thick $Pb(Mg_{1/3}Nb_{2/3})O_3$ films grown on $(100)_c SrRuO_3//(100)SrTiO_3$ and $(111)_c SrRuO_3//(111)SrTiO_3$ substrates.

Figs. 7 and 8 show the temperature dependencies of the saturation polarization ($P_{sat.}$) and the coercive field (Ec). As shown in Fig. 7, 1300 nm thick films showed larger $P_{sat.}$ and smaller Ec than 500 nm thick films in the overall temperature range for both (100) and (111)-oriented films. On the other hand, (111)-oriented films showed larger $P_{sat.}$ value than (100)-oriented one in the overall temperature range for both film thickness as shown in Fig. 8. The crystallographic

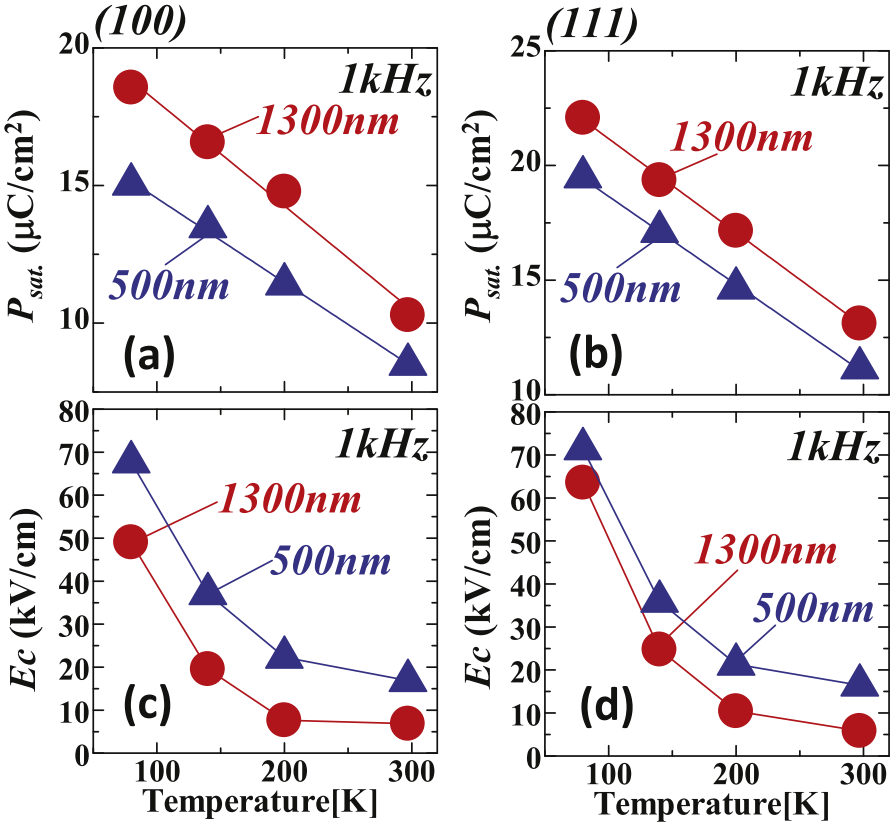

Fig. 7. Temperature dependencies of (a, b) saturation polarization ($P_{sat.}$) and (c, d) the coercive field (Ec) for $Pb(Mg_{1/3}Nb_{2/3})O_3$ films grown on (a, c) $(100)_c SrRuO_3//(100)SrTiO_3$ and (b, d) $(111)_c SrRuO_3//(111)SrTiO_3$ substrates.

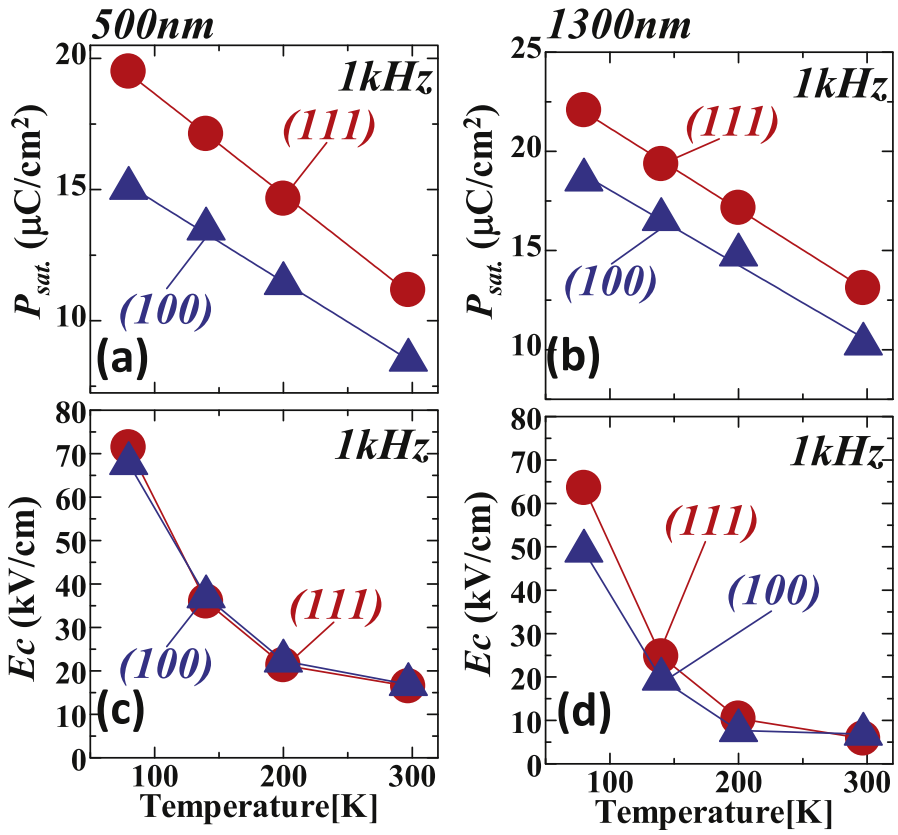

Fig. 8. Temperature dependencies of (a, b) saturation polarization ($P_{sat.}$) and (c, d) the coercive field (Ec) for (a, c) 500 nm-thick and (b, d) 1300 nm-thick $Pb(Mg_{1/3}Nb_{2/3})O_3$ films grown on $(100)_c SrRuO_3//(100)SrTiO_3$ and $(111)_c SrRuO_3//(111)SrTiO_3$ substrates.

relationship is also reported for the single crystal of $Pb(Mg_{1/3}Nb_{2/3})O_3$ that $P_{sat.}$ value of (111) is larger than that of (100) [15]. On the other hand, Ec value did not strongly depend on the film orientation. These results show that $P_{sat.}$ depends on both of film thickness and the film orientation and (111)-oriented films with 1300 nm thick show the maximum $P_{sat.}$ among present investigated four samples, whereas Ec does not depend strongly on the film orientation but on the film thickness. Film thickness dependency of $P_{sat.}$ must be taken into account of the piezoelectricity of $Pb(Mg_{1/3}Nb_{2/3})O_3$ films in addition to the discussion on the film thickness dependency of ε_r as discussed in Section 3.2. This is because larger electric field is applied to the film for $P-E$ hysteresis loop measurement and $Pb(Mg_{1/3}Nb_{2/3})O_3$ films are considered to have a relatively large piezoelectricity at low temperature. Based on these considerations, one possible reason is the film thickness dependency of the clamping effect from the substrate under applying an electric field. In fact, remanent polarization at electric field of 0 kV/cm does not show stronger thickness dependency than that of $P_{sat.}$.

4. Conclusion

Dielectric and ferroelectric properties of (100)- and (111)-oriented epitaxial $Pb(Mg_{1/3}Nb_{2/3})O_3$ films with 500 and 1300 nm in thickness grown by pulsed MOCVD were investigated as well as their crystal structure. Obvious crystal structure change with the film thickness was not observed and was almost the same with the reported data for bulk $Pb(Mg_{1/3}Nb_{2/3})O_3$. ε_r showed the frequency dependent maximum value against the temperature. ε_r(max.) and T(max.) decreased and increased with increasing frequency, respectively that are in good agreement with the reported data for the bulk. ε_r(max.) and T(max.) respectively increased and decreased with increasing the film thickness and (111)-oriented films showed larger value than (100) one. Ferroelectricity was observed for all films up to 297 K and monotonously decreased with increasing temperature. $P_{sat.}$ increased with increase of the film thickness and (111)-oriented films showed larger value than (100) one, while Ec decreased with increasing film thickness almost independent of the film orientation.

Acknowledgment

This work was supported by JSPS KAKENHI Grant Number 26220907 and 15H04121.

References

[1] Fu D, Taniguchi H, Itoh M, Koshihara S, Yamamoto N, Mori S. Relaxor $Pb(Mg_{1/3}Nb_{2/3})O_3$: a ferroelectric with multiple inhomogeneities. Phys Rev Lett 2009;103. 207601-1-4.

[2] Zhang S, Sherlock N, Meyer R, Shrout T. Crystallographic dependence of loss in domain engineered relaxor-PT single crystals. Appl Phys Lett 2009;94. 162906-1-3.

[3] Baek S, Park J, Kim D, Aksyuk V, Das R, Bu S, et al. Giant piezoelectricity on Si for hyperactive MEMS. Science 2011;334:958–61.

[4] Seo S, Kang H, Noh D, Yamada Y, Wasa K. Antiphase-type planar defects in $Pb(Mg_{1/3}Nb_{2/3-\delta})$ $O_3/SrTiO_3$ thin films. Appl Phys Lett 2004;84:3133–5.
[5] Nagarajan V, Ganpule C, Nagaraj B, Aggarwal S, Alpay S, Roytburd A, et al. Effect of mechanical constraint on the dielectric and piezoelectric behavior of epitaxial $Pb(Mg_{1/3}Nb_{2/3})$ O3(90%)–$PbTiO_3$(10%) relaxor thin films. Appl Phys Lett 1999;84:4183–5.
[6] Okamoto Sa, Yokoyama S, Okamoto Sh, Saito K, Uchida H, Koda S, et al. Strong dependence on thickness of room-temperature dielectric constant of (100)-oriented $Pb(Mg_{1/3}Nb_{2/3})O_3$ epitaxial films grown by metal organic chemical vapor deposition. Jpn J Appl Phys 2006;45:L1074–6.
[7] Streiffer S, Basceri C, Parker C, Lash S, Kingon A. Ferroelectricity in thin films: the dielectric response of fiber-textured $(Ba_xSr_{1-x})Ti_{1+y}O_{3+z}$ thin films grown by chemical vapor deposition. J Appl Phys 1999;86:4565–75.
[8] Yokoyama S, Honda Y, Morioka H, Okamoto S, Funakubo H, Iijima T, et al. Dependence of electrical properties of epitaxial $Pb(Zr,Ti)O_3$ thick films on crystal orientation and Zr/(Zr+Ti) ratio. J Appl Phys 2005;98. 094106-1-8.
[9] Xu R, Karthik J, Damodaran A, Martin L. Stationary domain wall contribution to enhanced ferroelectric susceptibility. Nat Commun 2014;5:3120. http://dx.doi.org/10.1038/ncomms4120. www.nature.com/naturecommunications.
[10] Nagashima K, Aratani M, Funakubo H. Improvement of property of $Pb(Zr_xTi_{1-x})O_3$ thin film prepared by source gas pulse-introduced metalorganic chemical vapor deposition. Jpn J Appl Phys 2000;39:L996–8.
[11] Higashi N, Watanabe T, Saito K, Yamaji I, Akai T, Funakubo H. Crystal structure comparison between conductive $SrRuO_3$ and $CaRuO_3$ thin films. J Cryst Growth 2001;229:450–6.
[12] Ismailzade I. Sov Phys Crystallogr 1960;5:292.
[13] Krainik NN, Kamzina LS, Smolenskii GA. Fiz Tverd Tela 1983;25:359. Sov. Phys. Solid State (English Transl.), 1983; 25: 202.
[14] Lanagan M, Yang N, Dube D, Jang S. Dielectric behavior of the relaxor $Pb(Mg_{1/3}Nb_{2/3})O_3$—$PbTiO_3$ solid-solution system in the microwave region. J Am Ceram Soc 1989;72:481–3.
[15] Schmidt G, Arndt H, Cieminski J, Petzsche T, Vogt H-J, Krainik NN. Krist Tech 1980;15:1415.

Professor Hiroshi Funakubo, Tokyo Institute of Technology. Dr. Hiroshi Funakubo is a professor of Department of Innovative and Engineered Materials, Tokyo Institute of Technology. He received the Ph. Dr. Degree from Tokyo Institute of Technology. In 1989, he was an assistant professor in the Faculty of Engineering, Tokyo Institute of Technology. In 1997 and 2012, he has been an associate professor and full professor of Interdisciplinary graduate school of Science and Technology, Department of Innovative and Engineering Materials, Tokyo Institute of Technology. His recent research focuses on preparation and properties of dielectric, ferroelectric and piezoelectric films. He has published over 500 papers in refereed international journals.

Mr. Satoshi Okamoto, Former student of Tokyo Institute of Technology. Satoshi Okamoto is a former student of Department of Innovative and Engineered Materials, Tokyo Institute of Technology. He received the master degree from Tokyo Institute of Technology. In 2006, he joins the company. He has published 7 papers in refereed international journals.

Dr. Shintaro Yokoyama, Former student of Tokyo Institute of Technology. Shinitaro Yokoyama is a former student of Department of Innovative and Engineered Materials, Tokyo Institute of Technology. He received the Ph. Dr. Degree from Tokyo Institute of Technology in 2006. He has published 60 papers in refereed international journals.

Mr. Shoji Okamoto, Former student of Tokyo Institute of Technology. Shoji Okamoto is a former student of Department of Innovative and Engineered Materials, Tokyo Institute of Technology. He received the master degree from Tokyo Institute of Technology. In 2005, he joins the company. He has published 30 papers in refereed international journals.

Dr. Junichi Kimura, Research Associate of Tokyo Institute of Technology. Junichi Kimura is a research associate of Department of Innovative and Engineered Materials, Tokyo Institute of Technology. He received the Ph. Dr. Degree from Tokyo Institute of Technology in 2015. He has published 9 papers in refereed international journals.

Professor Hiroshi Uchida, Sophia University. Dr. Hiroshi Uchida is an associate professor of Department of Materials and Life Sciences, Sophia University, Tokyo Japan. He received the Ph. Dr. Degree at Department on Inorganic Materials, Tokyo Institute of Technology, in 2000. His recent research focuses on chemical processing of metal-oxide thin films (*e.g.*, via sol–gel, chemical solution deposition and supercritical fluid deposition) for micro-/nano-electronics application. He has published over 100 papers in refereed international journals.